Journal of Materials Research and Technology 35 (2025) 6929–6938

Contents lists available at ScienceDirect

Journal of Materials Research and Technology

journal homepage: www.elsevier.com/locate/jmrt

Trade-off analysis of machinability of steel alloy AISI 304L using Taguchi-grey integrated approach

Faisal Abbas [a,1], Muhammad Ali Khan [b,c,1,2,*], Muhammad Iftikhar Faraz [d], Syed Husain Imran Jaffery [b,e], Sohail Akram [a], Jana Petru [f], Refka Ghodhbani [g,**], Walid M. Shewakh [h,i]

[a] Department of Mechanical Engineering (DME), Pakistan Institute of Engineering and Applied Sciences (PIEAS), Nilore, Islamabad, Pakistan
[b] School of Mechanical & Manufacturing Engineering (SMME), National University of Sciences & Technology (NUST), Islamabad, 44000, Pakistan
[c] Department of Mechanical Engineering, College of Electrical and Mechanical Engineering (CEME), National University of Sciences and Technology (NUST), Islamabad, 44000, Pakistan
[d] Department of Mechanical Engineering, College of Engineering, King Faisal University, Al-Ahsa, Saudi Arabia
[e] Department of Mechanical Engineering, College of Engineering, Faculty of Computing, Engineering and the Built Environment Birmingham City University, Birmingham, B4 7XG, UK
[f] Department of Machining, Assembly and Engineering Metrology, Mechanical Engineering Faculty, VSB-Technical University of Ostrava, 17, Listopadu 2172/15, Ostrava, 708 00, Czech Republic
[g] Center for Scientific Research and Entrepreneurship, Northern Border University, 73213, Arar, Saudi Arabia
[h] Department of Industrial Engineering, College of Engineering and Computer Sciences, Jazan University, Jazan, 82817, Saudi Arabia
[i] Mechanical Production Department, Faculty of Technology and Education, Beni-Suef University, P.O. Box 62521, Beni-Suef, 62511, Egypt

ARTICLE INFO

Handling editor: P Rios

Keywords:
AISI 304L
Stainless steel
Machining
Performance trade-offs
Optimization
Analysis of variance
Process analysis
Grey relational analysis
Regression analysis

ABSTRACT

Energy analysis during machine tool operations in manufacturing sector is becoming one of the prominent research avenues due to rising energy costs and environmental impact brought on by high energy consumption. Nevertheless, surface quality and production rates also hold significant value for overall optimization of any manufacturing setup. In fact, machinability of a material can only be assessed by collectively optimizing all machining responses. To address this shortcoming, multi-objective optimization of specific cutting energy, surface roughness, and material removal rate during turning of AISI 304L stainless steel was conducted at diverse machining parameters. Influential variables to include depth of cut, feed rate and cutting speed were taken as the input parameters. Efficient Taguchi design of experimentation was employed for formulation of L16 orthogonal array. Effect of each cutting parameter on the response variables was investigated using main effects plot and analysis of variance was done to ascertain influence of each input through its contribution ratio. Feed rate was found to be the most influential input with 88.94% contribution ratio for surface roughness and 57.29% contribution ratio for specific cutting energy. Cutting speed had contribution ratio of 31.56% for specific cutting energy. Subsequently, regression analysis was used to develop second-order mathematical models (95% confidence level) to correlate input parameters with output responses. Contour plots were developed for visual comprehension of the relationship between input parameters and output responses. Grey relational analysis was used for multi objective optimization to identify optimum cutting combination which came to be at 1.4 mm depth of cut, 160 m/min cutting speed and 0.25 mm/rev feed rate.

* Corresponding author. Department of Mechanical Engineering, College of Electrical and Mechanical Engineering (CEME), National University of Sciences and Technology (NUST), Islamabad, 44000, Pakistan.
** Corresponding author. Center for Scientific Research and Entrepreneurship, Northern Border University, 73213, Arar, Saudi Arabia.
E-mail addresses: mak.ceme@ceme.nust.edu.pk (M.A. Khan), Refka.Ghodhbani@nbu.edu.sa (R. Ghodhbani).
[1] These authors contributed equally to this work and are nominated as joint first authors.
[2] Current Address: Department of Mechanical Engineering, College of Electrical and Mechanical Engineering (CEME), National University of Sciences and Technology (NUST), Islamabad, 44000, Pakistan.

https://doi.org/10.1016/j.jmrt.2025.03.070
Received 9 February 2025; Received in revised form 4 March 2025; Accepted 7 March 2025
Available online 8 March 2025

1. Introduction

The fast growth of the manufacturing sector has greatly benefited human civilization while also escalating the issues of resource scarcity and environmental pollution [1]. Machine tools are the fundamental component of machining systems and have an enormous energy consumption. Data from the U.S energy yearbook [2] and related literature [3] suggests that the energy consumed in industrial setup contributes to 50% of the world's total energy consumption. Whereas out of the industrial energy breakdown, 90% of the total light manufacturing energy is expended in machining activities alone. Fossil fuels continue to be the main sources for energy creation despite the advancement of green energy technology. To fulfil the ever-increasing demands of industrial development, natural resources are being depleted quickly, which also contributes to an increase in carbon emissions. An adaptable, cost-effective, and environment friendly way to save energy is through its efficient consumption especially in the industrial setups. The concept of energy efficiency is not new, since due to rising energy costs, strict environmental regulations, and growing consumer awareness, energy efficiency has already become a top priority for the manufacturing sector during the past 20 years [4]. In this regard, many studies have been conducted on understanding and improving the energy consumption characteristics of the machine tools. However, a thorough research and use of structured methodologies for comprehending the machine tool energy characteristics for many materials is still inadequate [5,6].

In an effort to increase machine tool energy efficiency, several researchers have examined machine tools energy consumption characteristics using different materials. Vijayaraghavan et al. [7] reported that reducing machine tool energy usage can significantly enhance the manufacturing sector's environmental performance. Bagaber et al. [8] used response surface methodology (*RSM*) to undertake multi-objective optimization (*MOO*) of different response parameters including surface roughness (*Ra*), tool wear and power consumption while turning 316 stainless steel with an uncoated carbide cutting tool under dry cutting conditions. It was concluded that by employing the optimum cutting conditions, a reduction of 14.94%, 13.98% and 4.71% in surface roughness, tool wear and power consumption respectively. Khan et al. [9] aimed at identifying optimum cutting conditions corresponding to low tool wear, low Ra, and low SCE in turning of Titanium Alloy (Ti–6Al–4V) under cryogenic, dry, and wet conditions. It focused on MOO based on Grey Relational Analysis (*GRA*) using feed rate (f), cutting speed (v) and depth of cut (d) as input variables. The optimal cutting conditions resulted in an improvement of surface quality by 22% and tool wear by 30% and the energy used per unit volume decreased by 4%. Camposeco-Negrete et al. [10] used the Taguchi approach and Analysis of Variance (*ANOVA*) to optimize the cutting conditions when turning AISI 6061 T6 aluminum in order to reduce the energy consumption of the machine tool. The research showed that while a higher feed rate results in less energy being consumed, nevertheless it also results in increased surface *Ra*. Thus, it is important to realize that a set of cutting conditions that is optimal for one machining response may be the less suitable for another response. As a result, *MOO* is a more viable option than single-objective optimization. A tool-workpiece-based study [11] intending to analyze energy consumption during turning of Titanium alloy (Ti6Al4V) was carried out at different input cutting parameters. This study aimed to identify optimal cutting conditions conforming to the least amount of specific cutting energy (*SCE*) consumed which lead to significant energy savings. It was found that energy consumption was directly related with cutting speed and inversely related with f. In comparison, v was having much higher influence on energy consumption than f.

Masmiati et al. [12] used Response Surface Methodology (*RSM*) to predict the *Ra*, cutting force, and residual stress during machining of S50C medium carbon steel. Bhushan et al. [13] optimized the cutting parameters to minimize the machine tool energy consumption while maximizing the tool life. Saidi et al. [14] reported significance of employing optimal cutting parameters, based on desirability function, that influenced *Ra*, material removal rate (MRR) and tangential force to achieve quality and productivity. The study provided some insight into the relationship between *Ra* and productivity enhancement. Balaji et al. [15] carried out optimization of cutting parameters, namely *Ra* and tool vibrations, in drilling of AISI 304 stainless steel. DOE was based on Taguchi orthogonal array and the influence of parameters was analyzed through *ANOVA*. Du et al. [16] examined the energy consumption behavior in dry turning of AISI 304 and performed *MOO* involving three parameters namely microhardness, energy consumption and *Ra*. This study also used *ANOVA* and regression analysis to analyze the influence of cutting condition on responses and develop correlations. Ultra-high temperature (*UHT*) alloys were analyzed [17] through in-depth investigations, modeling and optimization during micro electro-discharge machining ($\mu - EDM$). Surface feature including effusion holes were researched using a copper-tungsten ($Cu-W$) hybrid tool electrode. Fault detection in glass fiber reinforced polymer was researched using recurrent neural networks (*RNN*) and modified particle swarm optimization (*mPSO*) techniques [18]. It was concluded that multiple transverse cracks can be predicted with more than 99% accuracy. Similarly in another study available in literature [19], analytical, finite element method, and neural network techniques were used to observe crack location and its depth resulting from fibre orientation effect in fibre-reinforced composites (*FRP*). *FRC* beams were also used in another research [20] for diagnosis of faults using artificial intelligence (*AI*) technique. It was seen that neuro-fuzzy hybrid technique can give accurate results. In another noteworthy work [21], position and extension of fault resulting from its natural frequency, mode shape curvature and fibre orientation is located in composite material structure. Fuzzy-neuro hybrid technique was employed for the purpose. Aluminium metal matrix composite (*AMMC*) beams were assessed [22] for cracks using finite element method in another significant work available in literature. Natural frequency and deferent mode shapes were analyzed to observe the behavior of *AMMC* beam structure.

A recent work [23] conducted turning of hardened AISI H13 with novel S3P-ALTiSiN coated carbide tool under minimum quantity lubrication conditions using cutting speed, nose radius, depth of cut, and feed as input variables. Tool life index was used to highlight the cost effectiveness of employed insert using Gilberts machining economic model. Tool nose radius was found to have 36.65% and 53.88% contribution ratios for Ra and tool vibration respectively. Hard turning of functionally graded specimen was carried out under Nanofluid-assisted minimum quantity lubrication (*NFMQL*) for analysis of surface integrity [24]. Taguchi L27 orthogonal array was formulated based on spindle speed, axial feed rate and depth of cut. The recommended machining conditions under *NFMQL* was shown to yield ecofriendly and sustainable manufacturing. Optimization through modeling of surface integrity during machining of AISI 4340 steel with coated ceramic tool was accomplished [25]. Response surface methodology was adopted to identify optimum cutting condition combination for ideal surface roughness. Parametric optimization using pressure, temperature and nozzle tip distance was achieved employing silicon carbide abrasive and quartz tool-workpiece interaction [26]. Grey relational analysis was used to optimize MRR and displacement of cut.

Realizing the significance of energy efficiency combined with its optimization along several other response parameters, this study undertook AISI 304L austenitic stainless steel for its *MOO* during turning. AISI 304/304L steel has well-known applications primarily because of its resistance to corrosion in structures, higher strength levels, varied fabrication properties, resistance to extreme temperatures as well as it being resistant to food-processing conditions, organic chemicals, dyestuffs, and a wide range of inorganic compounds [27]. It is also widely employed in storage of liquefied gases, cryogenic equipment, appliances, culinary equipment, medical equipment, transportation, waste-treatment plants, and other consumer items. AISI 304L, having less than 0.08% carbon, has additional fabrication applications due to its

weldability [28]. Although, rather relatively soft and highly ductile when annealed, austenitic stainless steels undergo substantial work hardening while being machined which can lead to excessive tool wear or even breakage [29]. Their high ductility renders it difficult to get good machining results. Poor chip breaking and formation of the build-up edge at the cutting face are both common occurrences. They adhere very strongly to the tool while being machined, and when a chip is formed, it can carry a part of the tool with it leading to an unpredictable tool wear performance [30]. Furthermore, as compared to other forms of stainless steels, austenitic steels ones have poor thermal conductivity which results in the building up of heat at the tool face readily. Consequently, their significant thermal expansion causes workpiece distortion or poor dimensional accuracy during machining [31,32]. The combination of these factors makes these steels difficult to machine. Numerous efforts have been undertaken to enhance the machinability of austenitic stainless steels [33]. Cutting parameter optimization is beneficial for producing highly precise and effective machining [34]. To investigate the relation among the cutting parameters and machining performance, various studies utilized the Taguchi technique and *ANOVA* as discussed previously and also reported by previous researchers. [35,36]. Furthermore, the GRA is frequently employed as an effective technique to carry out *MOO* of cutting conditions [37] considering both technical specifications and environmental performance.

Based on the aforementioned literature, it can be deduced that *MOO* has replaced single-objective optimization for collectively improving cutting parameters. For maximizing cutting performance, enhancing machined surface quality, lowering machining energy consumption, and raising productivity, the *MOO* of *Ra* in combination with *SCE* and *MRR* is very significant. For this reason, the present study constructs prediction models for *SCE*, *Ra*, and *MRR* and analyses the influence of cutting parameters on the three responses using *ANOVA*. It also focuses on *MOO* to contribute to sustainability, productivity and efficiency of machine tool machining for the AISI 304L stainless steel alloy. By investigating dry machining, which reduce the reliance on cutting fluids, this study promotes more sustainable and environmentally friendly manufacturing practices, aligning with the objectives of sustainable development goals.

2. Research motivation

Research motivation for this work was drawn from the need of collectively optimization of vital machining responses to enhance the prospects of sustainability and to improve the productivity and efficiency of machining processes. Currently no comprehensive research work is available regarding analysis of *SCE* consumption beyond 100 m/min *v*, in combination of other machining responses. The unavailability of such studies, based upon crucial outputs including *Ra*, *SCE* and *MRR* being representative of sustainability and productivity index of any machining system, is identified as a significant research gap. Hence research goals were selected based on formulation of comprehensive analysis of vital productivity and sustainability indices working with influential machining inputs. The contribution of envisioned work includes the study of individual and collective effects of input parameters on system output. Moreover, system productivity (*Ra and MRR*) and sustainability (*SCE*) is planned to be optimized through use of *MOO*. Intended work output is assumed to be of interest to various industries in general and manufacturing industry in particular. Machining of steel presents obstacles due to its low thermal conductivity and work hardening resulting in higher cutting temperatures as well as elevated cutting forces. This causes accelerated tool wear which amounts to higher machining costs and receded product surface integrity. The work also holds value due to the wide applications of AISI 304/304L stainless steel across number of industries including aerospace, medical, automotive and food processing owing to their high durability, biocompatibility and corrosion resistance.

3. Experimental details

In this study, an AISI 304L workpiece of 340 mm length, 220 mm outer diameter and 13 mm wall thickness was used for experimentation on a heavy duty YIDA ML-300 CNC turning center machine. Chemical composition of the workpiece material, found through XRF (X-ray fluorescence) analysis, and its mechanical properties are given in Tables 1 and 2 respectively. An aluminum mandrel fitted into the hollow workpiece was used to support it through the tailstock. Experimentation was carried out under dry conditions using PVD coated CNMG 120408 NN LT 10 cutting insert made by Lamina. The range of cutting conditions suggested by the manufacturer for this insert are; d = 0.5–5 mm, f = 0.2–0.4 mm/rev, and v = 170–270 m/min. The tool holder used is PCLNL2525 M12 by Walter. All the experiments were repeated twice using a fresh cutting edge each time to minimize experimental errors and ensure repeatability. Machine tool specifications are tabulated in Table 3. The workpiece setup is shown in Fig. 1.

3.1. Appearance and morphology

V, *d*, and *f* were chosen as input parameters whereas *Ra* and *SCE* were the measured response parameters. *MRR* was calculated analytically. *Ra* of the machined surface, after each experiment, was measured using Time-3110 *Ra* tester. The tester is placed at the machined surface for the roughness measurement, as shown in Fig. 2. As the sensitive probe at its bottom traverses horizontally, it also moves vertically to trace the surface irregularities. The movement from these irregularities is converted into electronic signals which are further converted and displayed in the form of roughness measurement values *Ra* or *Rz* (ten-point mean roughness).

To ensure that the error is kept to a minimum, the calibration of the tester was performed before taking the roughness measurements by making use of the calibration plate, as per instructions given in the manual. To reduce the influence of observational mistakes, three readings were recorded after each experiment. Each experimental run was repeated twice to further reduce the observational inconsistencies.

For *SCE* measurement, an authenticated two-cycle approach [38] was employed according to which two values of power, air cut power ($P-air$) and actual power ($P-actual$), are measured using a power measuring instrument. This approach has been employed in a number of other researches [39,40]. In the first cycle, $P-air$ is measured such that all the components of the machine are energized, and the cycle is performed under the required cutting conditions without performing the actual cutting process. In the second cycle, $P-actual$ is measured such that the tool is engaged with the workpiece performing the actual cutting process under the required cutting conditions. After the experimental measurements, the power consumed to remove the material during machining of the workpiece, the cutting power, *Pcut* (W), is measured using equation (1).

$$P_{cut} = P_{actual} - P_{air} \tag{1}$$

SCE ($J/mm3$), the energy required by the machine tool to remove a unit volume of the workpiece material, is then calculated by equation (2).

$$SCE = \frac{P_{cut}}{MRR} \tag{2}$$

Where material removal rate, *MRR* (mm^3/s), is given by equation (3).

$$MRR = v \times f \times d \tag{3}$$

In present study, the values of $P-air$ and $P-actual$ for each experiment were measured using Yokogawa CW 240 clamp-on power analyzer that measures 10 values of instantaneous power per second. Fig. 3 depicts the two-cycle approach showing $P-air$ and $P-actual$ values recorded by the power analyzer.

Table 1
Chemical composition of AISI 304L

Cr	Ni	Mn	Cu	C	Si	Zn	Mo	P	S	Fe
18.5	8.1	0.68	0.4	0.018	0.5	0.25	0.2	0.02	0.01	Balance

Table 2
Properties of AISI 304L

Density (g/cm^3)	Modulus of Elasticity (GPa)	Yield Strength (MPa)	Ultimate Tensile Strength (MPa)	Hardness (HB)	Elongation (%)	Thermal Conductivity (W/m. K)
8	193	215	505	123	70	16.2

Table 3
Machine tool specifications.

Machine Tool	Manufacturer	Spindle Power	Total Power	Max Speed	Max Turning Diameter
ML-300 Computer Numeric Control	YIDA Precision Machinery Company, Taiwan	15 kW	26 kW	3500 rpm	250 mm

3.2. Design of experiment

The DOE was based on the recommended cutting conditions range for stainless steels by the tool manufacturer and as reported in the literature [41,42] as given in Table 4. Taguchi design of experiments ($L16$), having four levels and three input parameters, given in Table 5, was employed for investigation of cutting conditions and the corresponding responses. This L16 experimental design array yields 16 rows and 3 columns based on which the responses were measured, as shown in Table 6. Dry cutting conditions were used in the trials as the benefits of using cutting fluids are not enunciated during high-speed machining as well as due to the concerns of sustainable metal cutting operations [43]. For the purpose of reducing error in the experimental data, the response to each cutting condition was measured twice.

4. Results and analysis

The response data collected for *Ra* and *SCE*, shown in Table 6, was analyzed using a number of techniques. *ANOVA* was employed to

Fig. 1. Workpiece setup.

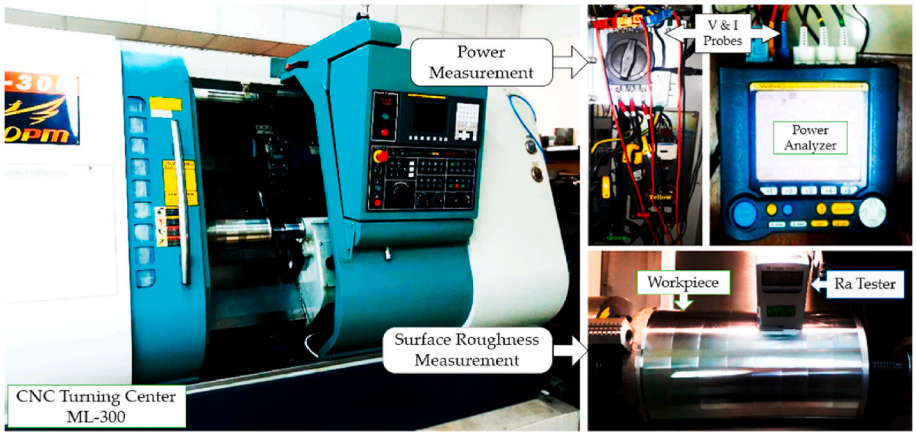

Fig. 2. Response measuring setup.

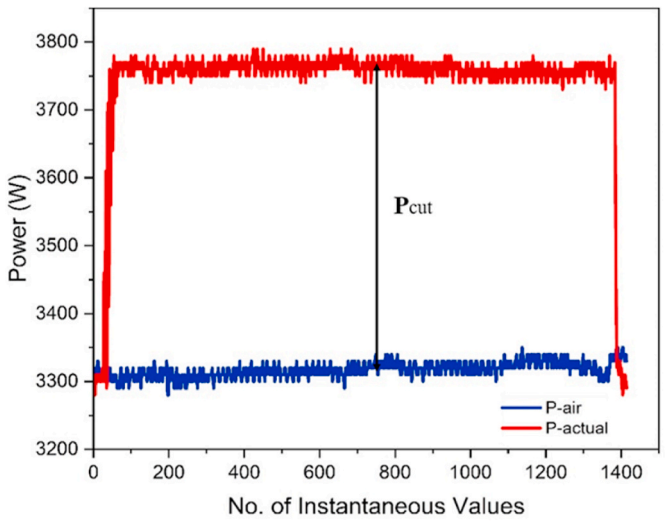

Fig. 3. Power consumption values for d = 1.5 mm, v = 80 m/min and f = 0.15mm/rev.

Table 4
Recommended cutting condition ranges.

Machining Parameter	Range
v (m/min)	50–300
f (mm/rev)	0.1–0.35
d (mm)	0.1–4

Table 5
Recommended cutting condition ranges.

Input Parameter	Level 1	Level 2	Level 3	Level 4
v (m/min)	80	120	160	200
f (mm/rev)	0.10	0.15	0.20	0.25
d (mm)	1	1.4	1.8	2.2

examine how much each input parameter influences the output response. The main effects plots were created to depict the trend of each response parameter under various cutting conditions. Then, the regression analysis was used to create second-order mathematical models that correlate the chosen input variables with the output responses. These models predict the output responses for various input parameter combinations without actually performing the experiments thus saving time and resources. Contour plots were created to have better visual observation of the relation between a response variable and two input variables. Finally, *GRA* was employed to carry out the *MOO* of the three responses by identifying the optimal parameter combination. Main effects plots and regression model for grey relational grade (*GRG*) were also developed to predict the collective output response for any number of input parameter combinations within the specified range.

4.1. Surface roughness

The effects of various input variables on *Ra* were assessed through *ANOVA* findings as shown in Table 7. Here it can be observed that input variables have different influence on output parameter. f is found to have the most notable effect on output response *Ra* with 88.94% contribution ratio followed by *v* (6.04%) and *d* (2.4%). This finding for *Ra* agree with a number of reported findings [44–46]. The dynamics of these occurrences were analyzed by examining the main effects plot.

The main effects plot for *Ra*, shown in Fig. 4, indicates that f has a highly increasing effect on *Ra* but it decreases with increase in v with relatively much lesser effect as compared to *f*. *d* has somewhat increasing effect on *Ra* but it stands insignificant. The high impact of *f* on *Ra* is mainly attributed to its geometric contribution since with increase in f, the peaks and crests of the machined surface are also increased in width [47]. Microgroove are imparted on the surface at elevated *f* which stretches and increases the surface roughness. Additionally, the increase in vibrations at the tool-workpiece interface due to higher f is also another reason for increased in *Ra* [48]. In case of *v*, *BUE* is developed at lower cutting speeds inducing chatter and degrading the surface roughness. *d* had an insignificant effect on surface integrity as shown in Fig. 4. The optimal value of *Ra* is attained at $v = 200$ m/min, $f = 0.10$ mm/rev and $d = 1.0$ mm.

Based on the experimental results for *Ra*, second-order mathematical model is developed at 95% confidence level and is given in equation (5). The presented model has its determination coefficient value $R2 = 97.38\%$, employing that it is a statistically significant and adequate

Table 7
ANOVA for Ra.

Source	DF	Seq SS	Adj SS	Adj MS	F-Value	P-Value	CR (%)
d	3	0.163	0.163	0.054	6.73	0.002	2.40
v	3	0.410	0.410	0.137	16.91	0.000	6.04
f	3	6.031	6.031	2.010	249.00	0.000	88.94
Error	22	0.178	0.178	0.008			2.62
Total	31	6.781					100.00

S = 0.0899 R-Sq = 97.38% R-Sq (Pred) = 94.46%.

Table 6
Experimental results.

Exp. No.	*D* (mm)	*V* (m/min)	*F* (mm/rev)	Ra (μm)		SCE (J/mm^3)		MRR (mm^3/s)
				Trial 1	Trial 2	Trial 1	Trial 2	
1	1	80	0.1	0.64	0.62	2.23	2.18	133
2	1	120	0.15	1.07	1.04	1.90	1.92	300
3	1	160	0.2	1.19	1.18	1.65	1.70	533
4	1	200	0.25	1.65	1.59	1.40	1.35	833
5	1.4	80	0.15	1.19	1.15	1.96	1.94	280
6	1.4	120	0.1	0.69	0.74	1.97	1.99	280
7	1.4	160	0.25	1.84	1.76	1.32	1.31	933
8	1.4	200	0.2	1.26	1.31	1.56	1.59	933
9	1.8	80	0.2	1.81	1.86	2.00	1.98	480
10	1.8	120	0.25	1.79	1.79	1.60	1.63	900
11	1.8	160	0.1	0.61	0.60	2.05	2.04	480
12	1.8	200	0.15	0.99	0.96	1.79	1.80	900
13	2.2	80	0.25	2.08	2.02	1.91	1.89	733
14	2.2	120	0.2	1.41	1.39	1.83	1.80	880
15	2.2	160	0.15	1.08	1.12	1.89	1.86	880
16	2.2	200	0.1	0.58	0.63	1.92	1.90	733

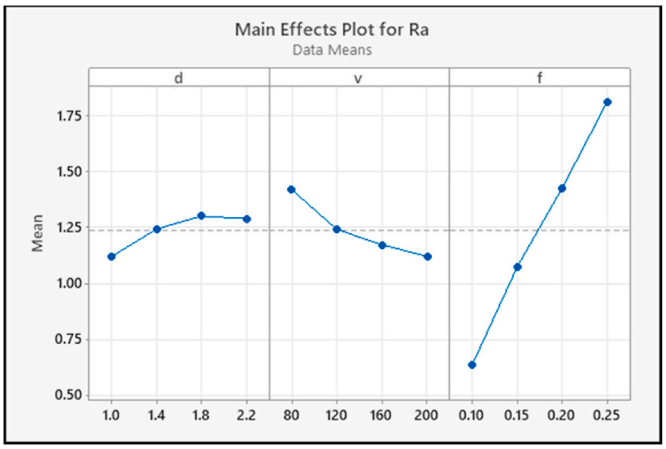

Fig. 4. Main effects plot for Ra.

model. Fig. 5 depicts the comparison of experimental roughness values and the predicted values based on the regression model (presented in equation (4)).

$$R_a = -0.991 + 1.226d - 0.00609v + 13.51f - 0.2103d^2 + 0.000020v^2 - 4.96f^2 - 0.00080d \times v - 1.929d \times f - 0.00827v \times f \quad (4)$$

The contour plot of *Ra* versus *v* and *f* is given in Fig. 6. Since *d* has an insignificant effect on *Ra*, no contour plot is generated to see its effect. The lighter portion of the plot represents lower values of roughness while the darker areas represent the higher *Ra* values. It can be seen that the regions get darker as the value of *f* increases; towards the bottom right of the plot. So, if better surface finish is to be obtained, the cutting parameters should be chosen such that they are from left and upper regions of the graph (lower *f* and higher *v*).

4.2. Specific cutting energy

SCE is an important machining response being indicative of system sustainability. Table 8 presents the analysis of variance results highlighting contribution ratios of individual input parameters. *SCE* is mainly dictated by f and v with 57.29% and 31.56% contribution ratios respectively. d has a relatively minute effect on *SCE* with a meagre 8.31% contribution ratio. Next, main effects plot are generated to better

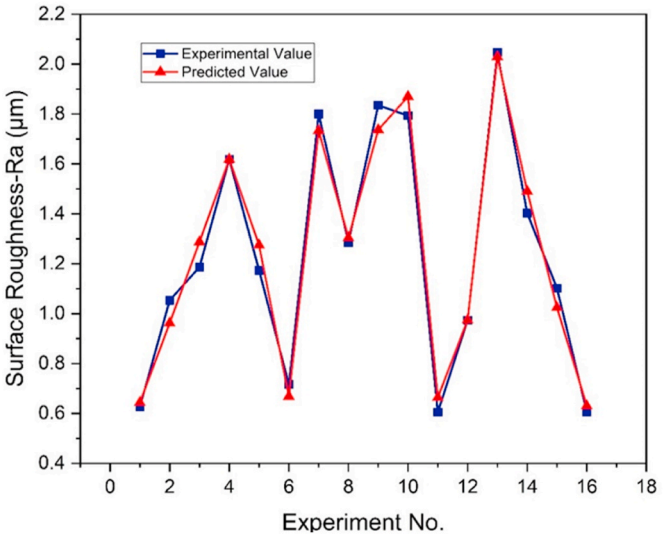

Fig. 5. Experimental vs Predicted values of Ra.

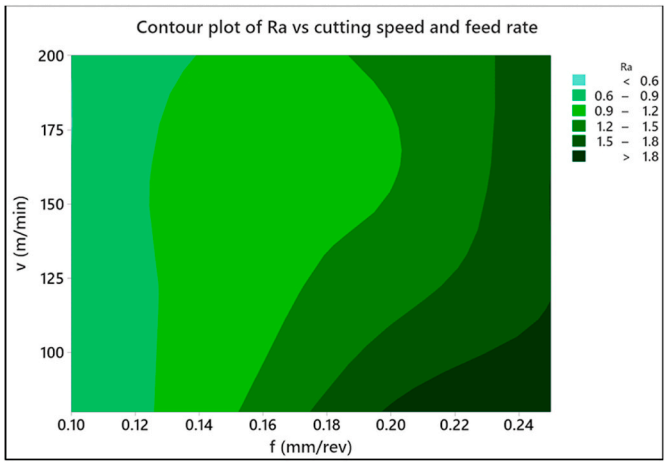

Fig. 6. Contour plot of Ra vs v and f.

Table 8
ANOVA for Ra.

Source	DF	Seq SS	Adj SS	Adj MS	F-Value	P-Value	CR (%)
d	3	0.145	0.145	0.048	21.44	0.000	8.31
v	3	0.552	0.552	0.184	81.46	0.000	31.56
f	3	1.002	1.002	0.334	147.84	0.000	57.29
Error	22	0.050	0.050	0.0023			2.84
Total	31	1.749					100.00

S = 0.0475 R-Sq = 97.16% R-Sq (Pred) = 93.99%.

comprehend the effects of input with their underlying mechanics of cutting.

The main effects plot for *SCE*, shown in Fig. 7, visually depicts the relative influence of each input parameter on *SCE*. A clear decreasing pattern is observed for SCE with increases in both *v* and *f*. *v* is directly related to the cutting zone temperature as concluded by Fan et al. [49] and Shaw [50]. With increase in cutting zone temperature at higher cutting speeds, the thermal softening effect is enhanced resulting in lower cutting forces and in turn lower *SCE*. Similarly, at higher feed rates, the amount of dissipating heat recedes [51] causing the cutting zone temperature to elevate. This results in lower *SCE* owing to greater thermal softening. The thermal softening occurs because of the lower thermal conductivity of the stainless-steel alloy due to which it gets heated up at high *v* and gets soften. This behavior is in line with other related studies [52,53]. Optimal cutting condition for *SCE* is observed to occur at $v = 200$ m/min, $f = 0.25$ mm/rev and $d = 1.4$ mm.

From the experimental findings for *SCE*, second-order mathematical

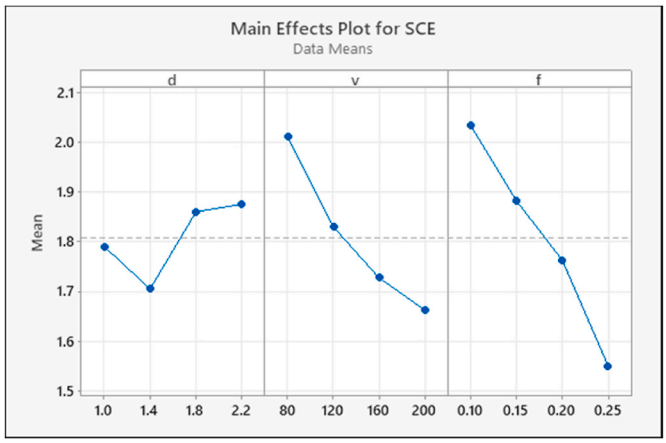

Fig. 7. Main effects plot for SCE.

model was generated as is given in equation (6). The presented model has $R2 = 96.48\%$, employing that it is a statistically significant and adequate model. Fig. 8 depicts the comparison of experimental *SCE* values and the predicted values based on the regression model (presented in equation (5)).

$$SCE = 2.765 - 0.404d - 0.00116v - 1.59f + 0.1575d^2 + 0.000018v^2 - 6.09f^2 - 0.002157d \times v + 1.339d \times f - 0.01559v \times f \quad (5)$$

The contour plot of *SCE* versus *v* and *f* is given in Fig. 9. Since again, *d* has an insignificant effect on *SCE*, contour plot including *d* is not plotted. It can be seen that the regions get lighter as the values of *v* and *f* increase; towards the right and upper portion of the plot. So, if lower *SCE* consumption is to be obtained, the cutting parameters should be chosen such that they are from the right and upper regions of the graph (higher *f* and higher *v*).

Based on the analysis, it can be concluded that the *SCE* decreases significantly as f rises, which is consistent with research findings made by Bagaber and Yusoff [8], according to which there is a negative association between energy consumption and f. A faster f will shorten the time needed to machine the material, which will lead to less energy consumption during cutting. Furthermore, in spite of the fact that high power is needed for high *v* and *f*, the *SCE* actually decreases as *v* and *f* increase. As demonstrated by work of Parida and Maity's [54], this result might be interpreted as indicating that the cutting force reduces as the *v* and *f* increase. The reason being that the contact time and friction time of the cutting zone are decreased as both these parameters rise. Meanwhile, thermal softening of the workpiece's surface also results in a decrease in the material's shear strength, which lowers the cutting force and subsequently the *SCE*. Additionally, as the *v* and *f* increase, the *MRR* also increases at even higher rates than the power consumption and since *SCE* is the ratio of power consumed and *MRR*, this reduces the actual *SCE* consumption. The analysis also revealed that *SCE* and *d* in the chosen range do not significantly correlate. As a result, choosing a higher *f* and *v* is critically important to reduce *SCE*.

5. Multi Objective Optimization

MOO deals with decision-making for problems that calls for the simultaneous optimization of various competitive and frequently incompatible objectives. The influence and relation between several parameters in a multi-response problem are intricate and somewhat ambiguous. This is stated as grey, which represents inaccurate and

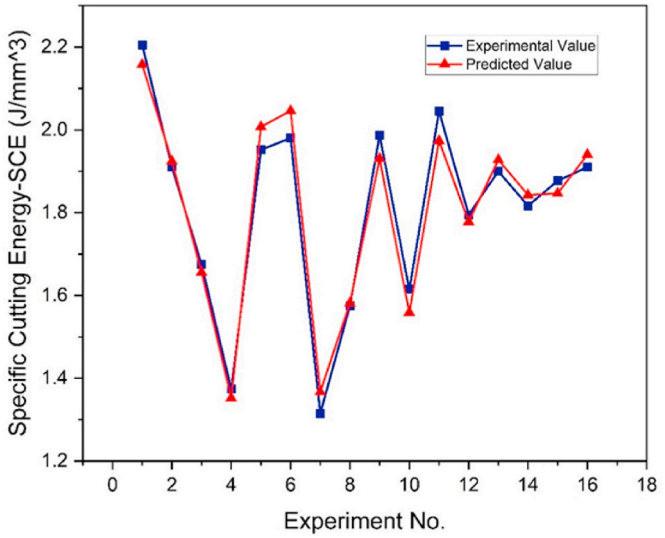

Fig. 8. Experimental vs Predicted values for SCE.

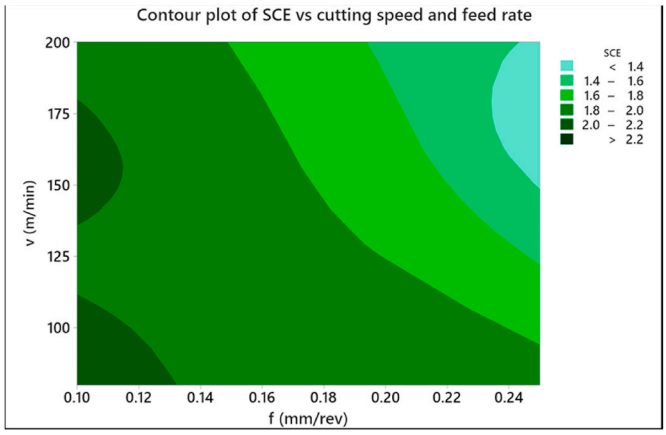

Fig. 9. Contour plot of SCE vs v and f.

ambiguous information. With the aid of grey relational grading, the *GRA* evaluates the complex uncertainty among the several responses in the given system and optimizes it. Consequently, a multi-response optimization problem is simplified to a single relational grade optimization problem which can then be ranked to obtain best and worst combination of input parameters [55]. In this study, *GRA* was performed using given below steps, whereas data is presented in Table 9.

5.1. Normalization of the data

First, preprocessing of Ra, SCE and MRR experimental results was performed to eliminate the impact of various units involved. Equation (6) was used to preprocess the original data sequence in case of Ra and SCE where it follows "smaller, the better" whereas, in case of MRR where it follows "the larger, the better". Equation (7) was used to preprocess and normalize the initial data.

All the equations used in GRA study were taken from study [56,57].

$$Z_{ij} = \frac{max\left(y_{ij}, i = 1, 2, \ldots.n\right) - y_{ij}}{\max\left(y_{ij}, i = 1, 2, \ldots.n\right) - \min\left(y_{ij}, i = 1, 2, \ldots.n\right)} \quad (6)$$

$$Z_{ij} = \frac{y_{ij} - \min\left(y_{ij}, i = 1, 2, \ldots.n\right)}{\max\left(y_{ij}, i = 1, 2, \ldots.n\right) - \min\left(y_{ij}, i = 1, 2, \ldots.n\right)} \quad (7)$$

Where y_{ij} represents the actual values of the responses, max $\left(y_{ij}\right)$ and min $\left(y_{ij}\right)$ are the highest and lowest values respectively for each

Table 9
Experimental results.

Sr. No.	Normalized Data			GRC			GRG	Rank
	Ra	SCE	MRR	Ra	SCE	MRR		
1	0.985	0.000	0.000	0.971	0.333	0.333	0.546	11
2	0.689	0.331	0.208	0.617	0.428	0.387	0.477	14
3	0.597	0.596	0.500	0.553	0.553	0.500	0.535	12
4	0.297	0.934	0.875	0.416	0.883	0.800	0.700	3
5	0.606	0.285	0.183	0.559	0.411	0.380	0.450	15
6	0.923	0.252	0.183	0.866	0.401	0.380	0.549	10
7	0.171	1.000	1.000	0.376	1.000	1.000	0.792	1
8	0.528	0.708	1.000	0.515	0.631	1.000	0.715	2
9	0.147	0.244	0.433	0.370	0.398	0.469	0.412	16
10	0.176	0.663	0.958	0.378	0.597	0.923	0.633	7
11	1.000	0.180	0.433	1.000	0.379	0.469	0.616	8
12	0.745	0.461	0.958	0.662	0.481	0.923	0.689	5
13	0.000	0.343	0.750	0.333	0.432	0.667	0.477	13
14	0.446	0.437	0.933	0.474	0.470	0.882	0.609	9
15	0.655	0.368	0.933	0.592	0.442	0.882	0.639	6
16	0.999	0.331	0.750	0.998	0.428	0.667	0.697	4

response whereas *Zij* represent the normalized values for each corresponding data set.

5.2. Grey relational coefficients calculation

In the next step, the normalized values were used to calculate the grey relational coefficients (*GRC*), which relates the ideal response value to the experimental value, using equation (8). GRG converts multiple *GRC* into a single combined factor.

$$\gamma(Z_o, Z_{ij}) = \frac{\Delta\min + \xi\Delta\max}{\Delta_{oj}(k) + \xi\Delta\max} \tag{8}$$

Where γ is the required GRC, Δmin and Δmax represent the smallest and largest values of the deviation sequence Δ*oj* and ξ is the distinguishing or identification coefficient. The distinguishing coefficient (ξ), has value ranging from 0 to 1. Usually and in this study, to assign equal weight to all the responses, the value of ξ was taken as 0.5. Otherwise, different weightage can be assigned to different response parameters as determined by manufacturer, based on customer requirement of the set policy. The deviation sequence is given by equation (9).

$$\Delta_{oj}(k) = \left|Z_o(k) - Z_{ij}(k)\right| \tag{9}$$

Where Zo(k) and Zij(k) represent the reference and comparability sequence respectively.

5.3. Grey relational coefficients calculation

After calculating GRCs, the grey relational grades (GRG) for each set of cutting conditions were calculated using equation (10).

$$GRG(Zo, Zij) = \frac{1}{n}\sum_{k=1}^{n}\gamma(Zo, Zij) \tag{10}$$

Where n is the number of response variables. GRG is the overall representative of the quality characteristics. Maximizing the obtained grey relationship grade will yield the optimum results.

5.4. Rank calculation

The final step was to rank all the experiments from 1 to 16 as per their corresponding *GRG* values such that the one having maximum value of *GRG* is ranked 1 and the one having minimum value of *GRG* is ranked 16. The experimental run having the rank 1 was chosen as having optimal parametric combination for multi-responses.

The data is tabulated in Table 9 based on the four steps given above.

Experiment no. 7, with input cutting conditions of $d = 1.4$ mm, $v = 160$ m/min and $f = 0.25$ mm/rev, has the highest value of *GRG* which means that this combination of cutting condition is ideal for simultaneous optimization of the machining process. A mathematical model (R2 = 97.38%) was also generated for predicting *GRG* values for any combination of input parameters. The model is given in equation (11) while the comparison between experimental and predicted *GRG* values based on this model is presented in Fig. 10.

$$GRG = 1.289 - 0.167d - 0.00343v - 7.70f - 0.0688\,d^2 - 0.000006v^2 + 12.10\,f^2 + 0.002419d \times v + 0.940\,d \times f + 0.02109v \times f \tag{11}$$

6. Conclusion

In the current research, effects of vital machining input were analyzed in terms of output responses during turning of 304L stainless steel under dry conditions. Analysis of variance, main effects plot and contour plots were used to quantify the influence of each input. Subsequently, collective optimization of responses was conducted using grey relational analysis. Following conclusions were drawn during the course of the work.

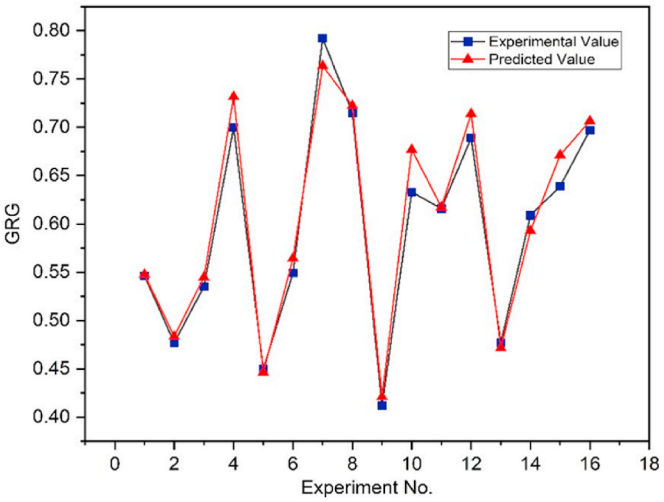

Fig. 10. GRG -Experimental vs Predicted.

1. Analysis of variance of *Ra* identified *f* as the most influential with 88.94% contribution ratio followed by *v* with 6.04% contribution ratio. *d* was found to be insignificant.
2. Change in *v* and *f* were found to have opposite effects on *Ra* with *v* inversely and *f* directly proportional to Ra. Optimum value for *Ra* is valued to be at 200 m/min *v*, 0.1 mm/rev *f* and 1.0 mm *d*.
3. Contour plot marked low *f* and high *v* was as the desired combination for improved *Ra* values.
4. In case of *SCE*, *f* and *v* were seen to be significant with 57.29% and 31.56% contribution ratios.
5. *SCE* was found to decrease with increase in both *v* and *f* owing to the thermal softening effects associated with higher cutting zone temperature. *SCE* was seen to optimize at 200 m/min *v*, 0.25 mm/rev *f* and 1.4 mm *d*.
6. Optimum values of *SCE* were observed to occur at high *v* and high *f* combinations as highlighted by contour plot.
7. Regression models developed for *SCE* and *Ra* level had determination coefficients 96.48% and 97.38% respectively. whereas determination coefficient for *GRG* regression model came out to be 97.38% developed at 95% confidence level.
8. Based on GRA, run no 7 at 160 mm/min *v*, 0.25 mm/rev *f* and 1.4 mm *d* was measured to be the optimal combination of input parameters for collective optimization of system sustainability and productivity.

Author contributions

Conceptualization, Faisal Abbas, Sohail Akram, Muhammad Ali Khan, Husain Imran Jaffrey, Jana Petru, Refka Ghodhbani and Walid M. Shewakh; Data curation, Faisal Abbas, Sohail Akram, Muhammad Ali Khan, Muhammad Iftikhar Faraz, Husain Imran Jaffrey, Jana Petru, Refka Ghodhbani and Walid M. Shewakh; Formal analysis, Faisal Abbas, Sohail Akram, Muhammad Ali Khan, Muhammad Iftikhar Faraz, Husain Imran Jaffrey, Jana Petru, Refka Ghodhbani and Walid M. Shewakh; Investigation, Faisal Abbas, Sohail Akram, Muhammad Ali Khan, Muhammad Iftikhar Faraz, Husain Imran Jaffrey, Jana Petru and Walid M. Shewakh; Methodology, Faisal Abbas, Sohail Akram, Muhammad Ali Khan, Muhammad Iftikhar Faraz, Husain Imran Jaffrey, Jana Petru and Refka Ghodhbani; Resources, Refka Ghodhbani; Software, Faisal Abbas, Muhammad Ali Khan, Muhammad Iftikhar Faraz, Husain Imran Jaffrey and Walid M. Shewakh; Supervision, Sohail Akram, Muhammad Ali Khan and Husain Imran Jaffrey; Validation, Faisal Abbas, Sohail Akram,

Muhammad Ali Khan, Muhammad Iftikhar Faraz, Jana Petru, Refka Ghodhbani and Walid M. Shewakh; Writing – original draft, Faisal Abbas, Sohail Akram, Muhammad Ali Khan, Muhammad Iftikhar Faraz, Husain Imran Jaffrey, Jana Petru, Refka Ghodhbani and Walid M. Shewakh; Writing – review draft, Faisal Abbas, Sohail Akram, Muhammad Ali Khan, Muhammad Iftikhar Faraz, Husain Imran Jaffrey, Jana Petru, Refka Ghodhbani and Walid M. Shewakh.

Institutional review board statement

Not applicable.

Data availability statement

The original contributions presented in this study are included in the article. Further inquiries can be directed to the corresponding author.

Funding

This article was co-funded by the European Union under the REFRESH – Research Excellence For REgion Sustainability and High-tech Industries project number CZ.10.03.01/00/22_003/0000048 via the Operational Programme Just Transition.

Declaration of competing interest

The authors declare that they have no known competing financial interests or personal relationships that could have appeared to influence the work reported in this paper.

Acknowledgments

This work was supported by the Deanship of Scientific Research, Vice Presidency for Graduate Studies and Scientific Research, King Faisal University, Saudi Arabia (Grant No. KFU250958). The authors extend their appreciation to the Deanship of Scientific Research at Northern Border University, Arar, KSA for funding this research work through the project number "NBU-FPEJ-2025-2461-03."

References

[1] Zhao GY, Liu ZY, He Y, Cao HJ, Guo YB. Energy consumption in machining: Classification, prediction, and reduction strategy. 2017. https://doi.org/10.1016/j.energy.2017.05.110.
[2] Ratner M, Glover C. US energy: Overview and key statistics. https://sgp.fas.org/crs/misc/R40187.pdf. [Accessed 3 March 2025].
[3] Khan MA, Imran Jaffery SH, Khan M, Alruqi M. Machinability analysis of Ti-6Al-4V under cryogenic condition. J Mater Res Technol 2023;25:2204–26. https://doi.org/10.1016/j.jmrt.2023.06.022.
[4] Teja D, Muvvala P, Nittala N, Bandhu D, K M, Energy, and undefined. Comparative performance analysis of recuperative helium and supercritical CO_2 Brayton cycles for high-temperature energy systems. ElsevierDVH Teja, P Muvvala, N. Nittala, D Bandhu, MI Khan, KK Saxena, MI KhanEnergy, 2024•Elsevier, https://www.sciencedirect.com/science/article/pii/S0360544224032456. [Accessed 5 March 2025].
[5] Khan MA, Jaffery SHI, Baqai AA, Khan M. Comparative analysis of tool wear progression of dry and cryogenic turning of titanium alloy Ti-6Al-4V under low, moderate and high tool wear conditions. Int J Adv Manuf Technol Jul. 2022;121(1–2):1269–87.
[6] Sulochana G, Prasad C, Bhatti S, V. M, Energy, and undefined. Impact of multi-walled carbon nanotubes (MWCNTs) on hybrid biodiesel blends for cleaner combustion in CI engines. https://www.sciencedirect.com/science/article/pii/S0360544224016840. [Accessed 5 March 2025].
[7] Vijayaraghavan A, Dornfeld D, Vijayaraghavan A, Dornfeld D. Automated energy monitoring of machine tools. Elsevier 2010;59:21–4. https://doi.org/10.1016/j.cirp.2010.03.042.
[8] Bagaber S, A. Y.-J. of cleaner production, and undefined. Multi-objective optimization of cutting parameters to minimize power consumption in dry turning of stainless steel 316. J Clean. Prod 2017. Available: https://www.sciencedirect.com/science/article/pii/S0959652617306753. [Accessed 3 March 2025].
[9] Khan MA, et al. Multi-objective optimization of turning titanium-based alloy Ti-6Al-4V under dry, wet, and cryogenic conditions using gray relational analysis (GRA). Int J Adv Manuf Technol Feb. 2020;106(9–10):3897–911. https://doi.org/10.1007/S00170-019-04913-6.
[10] C. C.-N.-J. of cleaner production and undefined. Optimization of cutting parameters for minimizing energy consumption in turning of AISI 6061 T6 using Taguchi methodology and ANOVA. Camposeco-Negrete J Clean. Prod 2013. https://www.sciencedirect.com/science/article/pii/S095965261300187X. [Accessed 3 March 2025].
[11] Khan MA, Jaffery SHI, Khan M. Assessment of sustainability of machining Ti-6Al-4V under cryogenic condition using energy map approach. Eng. Sci. Technol. an Int. J. May 2023;41:101357.
[12] Masmiati N, Sarhan AAD, Hassan MAN, Hamdi M. Optimization of cutting conditions for minimum residual stress, cutting force and surface roughness in end milling of S50C medium carbon steel. Meas. J. Int. Meas. Confed. 2016;86:253–65.
[13] Bhushan RK. Optimization of cutting parameters for minimizing power consumption and maximizing tool life during machining of Al alloy SiC particle composites. J Clean Prod 2013;39:242–54. https://doi.org/10.1016/j.jclepro.2012.08.008.
[14] Saidi R, Ben Fathallah B, Mabrouki T, Belhadi S, Yallese MA. Modeling and optimization of the turning parameters of cobalt alloy (Stellite 6) based on RSM and desirability function. Int J Adv Manuf Technol Feb. 2019;100(9–12):2945–68. https://doi.org/10.1007/S00170-018-2816-X.
[15] Balaji M, Murthy B, R.-P N, Technology, and undefined. Optimization of cutting parameters in drilling of AISI 304 stainless steel using Taguchi and ANOVA. Proced Technol 2016. https://www.sciencedirect.com/science/article/pii/S2212017316305710. [Accessed 3 March 2025].
[16] Du F, He L, Huang H, Zhou T, W J, Materials, and undefined. Analysis and multi-objective optimization for reducing energy consumption and improving surface quality during dry machining of 304 stainless steel. Mater 2020. https://doi.org/10.3390/ma13214693.
[17] Dhupal D, et al. Generation of effusion holes on ultra-high temperature alloy by micro electro-discharge machining process. Surf Rev Lett Feb. 2024;31(2). https://doi.org/10.1142/S0218625X2450015X.
[18] Parida SP, Sahoo S, Jena PC. Prediction of multiple transverse cracks in a composite beam using hybrid RNN-mPSO technique. Proc Inst Mech Eng Part C J Mech Eng Sci Aug. 2024;238(16):7977–86. https://doi.org/10.1177/09544062241239415.
[19] Jena PC, Parhi DR, Pohit G. Dynamic investigation of FRP cracked beam using neural network technique. J. Vib. Eng. Technol. Dec. 2019;7(6):647–61. https://doi.org/10.1007/S42417-019-00158-5.
[20] P. J.-M. T, Proceedings and undefined. Fault assessment of FRC cracked beam by using neuro-fuzzy hybrid technique. Mater Today: Proceed 2018. https://www.sciencedirect.com/science/article/pii/S2214785318314007. [Accessed 4 March 2025].
[21] D. R. Jena, Pankaj Charan; Pohit, Goutam; Parhi, Fault Measurement in Composite Structure by Fuzzy-Neuro Hybrid Technique from the Natural Frequency and Fibre Orientation.
[22] Jena P, Parhi D, Pohit G, B. S.-M. T, Proceedings, and undefined. Crack assessment by FEM of AMMC beam produced by modified stir casting method. Mater Today Proceed 2015. https://www.sciencedirect.com/science/article/pii/S2214785315005088. [Accessed 4 March 2025].
[23] Mahapatra S, Das A, Jena PC, Das SR. Turning of hardened AISI H13 steel with recently developed S3P-AlTiSiN coated carbide tool using MWCNT mixed nanofluid under minimum quantity lubrication. Proc Inst Mech Eng Part C J Mech Eng Sci Feb. 2023;237(4):843–64. https://doi.org/10.1177/09544062221126357.
[24] Pradhan S, Das SR, Jena PC, Dhupal D. Investigations on surface integrity in hard turning of functionally graded specimen under nano fluid assisted minimum quantity lubrication. Adv. Mater. Process. Technol. 2022;8(sup3):1714–29. https://doi.org/10.1080/2374068X.2021.1948706.
[25] Jena J, Panda A, Behera AK, Jena PC, Das SR, Dhupal D. Modeling and optimization of surface roughness in hard turning of AISI 4340 steel with coated ceramic tool. Innov. Mater. Sci. Eng. 2019:151–60. https://doi.org/10.1007/978-981-13-2944-9_15.
[26] Pradhan S, Tripathy S, Sahu S, S. D.-M. T, undefined. Investigation on MRR and DOC of the micro-holes generated on quartz using silicon carbide by FB-HAJM. Mater Today Proceed 2020. https://www.sciencedirect.com/science/article/pii/S2214785320311925. [Accessed 4 March 2025].
[27] Toronto AS-NI, undefined ON, undefined Canada, and undefined. Design guidelines for the selection and use of stainless steels. Ser Inst 2020 [Online]. Available: https://nickelinstitute.org/media/4664/ni_aisi_9014_selectionuse.pdf. [Accessed 3 March 2025].
[28] He Q, Jin Z, Jiang G, Shi Y. The investigation on electrochemical denatured layer of 304 stainless steel. Mater Manuf Process Nov. 2018;33(15):1661–6. https://doi.org/10.1080/10426914.2018.1453152.
[29] Korkut I, Kasap M, Ciftci I, U. S.-M, Design, and undefined. Determination of optimum cutting parameters during machining of AISI 304 austenitic stainless steel. Mater Des 2004. https://www.sciencedirect.com/science/article/pii/S0261306903002292. [Accessed 3 March 2025].
[30] Ahmad A, Akram S, Jaffery SHI, Khan MA. Evaluation of specific cutting energy, tool wear, and surface roughness in dry turning of titanium grade 3 alloy. Int J Adv Manuf Technol Jul. 2023;127(3–4):1263–74. https://doi.org/10.1007/S00170-023-11580-1.
[31] Ali Khan M, Husain Imran Jaffery S, Khan M, Ikramullah Butt S. Wear and surface roughness analysis of machining of Ti-6Al-4V under dry, wet and cryogenic conditions. In: IOP Conference Series: materials Science and Engineering; 2019. p. 561–73.
[32] Ahmad A, Khan M, Akram S, Faraz M, S. J.-R, in, and undefined. Achieving sustainable machining of titanium grade 3 alloy through optimization using grey

relational analysis (GRA). Res Eng 2024. https://www.sciencedirect.com/science/article/pii/S2590123024006108. [Accessed 16 June 2024].
[33] O'sullivan D, M. C.-J. of materials processing technology, and undefined. Machinability of austenitic stainless steel SS303. J. Mater Process Technol 2002. https://www.sciencedirect.com/science/article/pii/S0924013602001978. [Accessed 3 March 2025].
[34] Sheheryar M, et al. Multi-objective optimization of process parameters during micro-milling of Nickel-based alloy Inconel 718 using Taguchi-grey relation integrated approach. Materials Nov. 2022;15(23):8296. https://doi.org/10.3390/MA15238296. 2022, Vol. 15, Page 8296.
[35] Siddique M, Faraz M, Butt S, Khan R, P J, Machines, and undefined. Parametric analysis of tool wear, surface roughness and energy consumption during turning of Inconel 718 under dry, wet and MQL conditions. Machines 2023. https://www.mdpi.com/2075-1702/11/11/1008. [Accessed 16 June 2024].
[36] Rauf A, Khan M, Jaffery S, S. B.-J. of M. R. and, and undefined. Effects of machining parameters, ultrasonic vibrations and cooling conditions on cutting forces and tool wear in Meso Scale Ultrasonic vibrations assisted. J Mater. Res. Technol 2024. https://www.sciencedirect.com/science/article/pii/S2238785424012420. [Accessed 16 June 2024].
[37] Zaidi S, Qadir NU, Jaffery S, Khan M, K M, Materials, and undefined. Statistical analysis of machining parameters on burr formation, surface roughness and energy consumption during milling of aluminium alloy Al 6061-T6. J Petru Mater 2022 [Online]. Available: https://www.mdpi.com/1996-1944/15/22/8065. [Accessed 16 June 2024].
[38] Raza Zaidi S, Ikramullah Butt S, Ali Khan M, Iftikhar Faraz M, Husain Imran Jaffery S, Petru J. Sustainability assessment of machining Al 6061-T6 using Taguchi-grey relation integrated approach. Heliyon 2024:e33726. https://doi.org/10.1016/j.heliyon.2024.e33726.
[39] Khan M, Jaffery S, M. K.-2020 I. 11th, and undefined. Sustainability analysis of turning aerospace alloy Ti-6Al-4V under dry, wet and cryogenic conditions. IEEE 11th Int Conf Mech 2020 [Online]. Available: https://ieeexplore.ieee.org/abstract/document/9041160/. [Accessed 3 March 2025].
[40] Khan M, Letters SM-M, undefined. Tool chip contact length analysis of dry and cryogenic turning of aerospace alloy Ti-6Al-4V. Elsevier; 2024 [Online]. Available: https://www.sciencedirect.com/science/article/pii/S2213846324001469. [Accessed 3 March 2025].
[41] Groover Mikell P. Fundamentals of Modern Manufacturing Materials, Processes, and Systems Seventh Edition. 2020.
[42] Kalpakjian S, Schmid SR. Manufacturing engineering and technology. Upper Saddle River, NJ, USA: Pearson; 2014.
[43] Fratila D, C. C.-J. of cleaner production, and undefined. Application of Taguchi method to selection of optimal lubrication and cutting conditions in face milling of AlMg3. Frat. J Clean Prod 2011 [Online]. Available: https://www.sciencedirect.com/science/article/pii/S0959652610004592. [Accessed 3 March 2025].
[44] Das S, Panda A, D. D.-M. of A. M. and, and undefined. Experimental investigation of surface roughness, flank wear, chip morphology and cost estimation during machining of hardened AISI 4340 steel with coated carbide. Adv. Mater. Mod. Process 2017;3(1). https://doi.org/10.1186/s40759-017-0025-1.
[45] Xavior M, M. A.-J, of materials processing technology, and undefined. Determining the influence of cutting fluids on tool wear and surface roughness during turning of AISI 304 austenitic stainless steel. Elsevier, https://www.sciencedirect.com/science/article/pii/S0924013608002094. [Accessed 3 March 2025].
[46] Khan MA, et al. Statistical analysis of energy consumption, tool wear and surface roughness in machining of Titanium alloy (Ti-6Al-4V) under dry, wet and cryogenic conditions. Mech Sci 2019;10:561–73. https://doi.org/10.5194/ms-10-561-2019.
[47] Mia M, D N, Measurement, and undefined. Prediction of surface roughness in hard turning under high pressure coolant using Artificial Neural Network. Measurement 2016 [Online]. Available: https://www.sciencedirect.com/science/article/pii/S0263224116303402. [Accessed 3 March 2025].
[48] Yan J, Li L. Multi-objective optimization of milling parameters-the trade-offs between energy, production rate and cutting quality. J Clean Prod 2013;52:462–71. https://doi.org/10.1016/j.jclepro.2013.02.030.
[49] Fan Y, Hao Z, Zheng M, Yang S. Wear characteristics of cemented carbide tool in dry-machining Ti-6Al-4V. Mach Sci Technol Apr. 2016;20(2):249–61. https://doi.org/10.1080/10910344.2016.1165837.
[50] Shaw MC. In: Metal cutting Principles. second ed. Oxford University Press; 2005.
[51] Sarwar M, Persson M, Hellbergh H, Haider J. Measurement of specific cutting energy for evaluating the efficiency of bandsawing different workpiece materials. Int J Mach Tool Manufact 2009;49(12–13):958–65.
[52] Akram S, Jaffery SHI, Khan M, Fahad M, Mubashar A, Ali L. Numerical and experimental investigation of Johnson–Cook material models for aluminum (AL 6061-t6) alloy using orthogonal machining approach. Adv Mech Eng 2018;10(9):1–14.
[53] Akram S, Jaffery SHI, Anwar Z, Khan M, Khan MA. Toward clean manufacturing: an analysis and validation of a modified Johnson–Cook material model for low and high-speed orthogonal machining of low-carbon aluminum alloy (Al 6061-T6). Int J Adv Manuf Technol Nov. 2023;129(5–6):2523–36. https://doi.org/10.1007/S00170-023-12367-0.
[54] Parida A, K. M, Measurement, and undefined. Numerical and experimental analysis of specific cutting energy in hot turning of Inconel 718. Measurement 2019. https://www.sciencedirect.com/science/article/pii/S0263224118309709. [Accessed 3 March 2025].
[55] Panda A, Sahoo A, Lett AR-DS, undefined. Multi-attribute decision making parametric optimization and modeling in hard turning using ceramic insert through grey relational analysis: a case study. Sci Lett 2016;5:581–92. https://doi.org/10.5267/j.dsl.2016.3.001. 2016.
[56] Khan M, Khan M, Aziz S, Faraz M, A. T.-A, Sciences, and undefined. Experimental evaluation of surface roughness, burr formation, and tool wear during micro-milling of titanium grade 9 (Ti-3Al-2.5 V) using statistical evaluation. Appl Sci 2023. https://www.mdpi.com/2076-3417/13/23/12875. [Accessed 3 March 2025].
[57] Khan MA, Jaffery SHI, Khan MA, Faraz MI, Mufti S. Multi-objective optimization of micro-milling titanium alloy Ti-3Al-2.5V (Grade 9) using Taguchi-grey relation integrated approach. Metals 2023;13(8).